Published in final edited form as:
Biochem J. 2014 March 15; 458(3): 575–583. doi:10.1042/BJ20121546.

Effects of alternative splicing on function of Bestrophin-1 calcium-activated chloride channels

Yu-Hung Kuo[*], **Iskandar F. Abdullaev**[†], **María C. Hyzinski-García**[†], and **Alexander A. Mongin**[†,1]

[*]Division of Neurosurgery, Department of Surgery, Albany Medical College, Albany, NY 12208, U.S.A.

[†]Center for Neuropharmacology and Neuroscience, Albany Medical College, Albany, NY 12208, U.S.A.

Synopsis

The proposed Ca^{2+}-activated Cl^- channel protein Bestrophin 1 (Best1) is expressed and functionally important in the retina and in the brain. Human *BEST1* has two known splice variants, Best1V1 and Best1V2, which arise from alternative splicing of two exons: exon 2 splicing results in a unique N-terminal domain, whereas alternative splicing of exon 11 produces two mutually exclusive C-termini. Prior studies were limited to Best1V1 and its clinically relevant mutations. In the present work, we cloned a novel splice variant of Best1V1 missing exon 2 (Best1V1Δex2) and differing from each of the two previously identified isoforms by one alternatively spliced domain. This finding allowed us to determine the role for alternative splicing of the Best1 N- and C-termini. We heteroexpressed Best1V1Δex2 in HEK293 cells, and compared its properties to Best1V1 and Best1V2. Western blot analysis confirmed protein expression from all three splice variants. Both Best1V1 and Best1V1Δex2 successfully formed Ca^{2+}-activated Cl^- channels, demonstrating that the N-terminus encoded by exon 2 is not essential for channel function. In contrast, Best1V2 expressing cells had no detectable Ca^{2+}-activated Cl^- currents, pointing to a critical role for splicing of the C-terminus. Surface protein biotinylation demonstrated that Best1V1 and Best1V1Δex2 are trafficked to the plasma membrane, whereas Best1V2 is not. These results define the impact of alternative splicing on Best1 function, and should be taken into consideration in future modeling of the Best1 protein structure.

Keywords

chloride channels; Bestrophins; VMD2; splicing; glioblastoma multiforme; astrocytes

[1]To whom correspondence should be addressed: Tel. (518) 262-9052; Fax (518) 262-5799; MonginA@mail.amc.edu.

Summary Statement: Missense mutations in the chloride channel Bestrophin-1 have been linked to diseases of visual system. We cloned and characterized novel splice variant of Bestrophin-1; and found that it unexpectedly retains chloride channel function despite missing the first predicted transmembrane domain.

Author Contribution: Yu-Hung Kuo, Iskandar F. Abdullaev, and Alexander A. Mongin designed experiments and analyzed the data. Yu-Hung Kuo, Iskandar F. Abdullaev, and María C. Hyzinski-García conducted experiments. Yu-Hung Kuo and Alexander A. Mongin wrote the paper.

Introduction

The Bestrophin family is composed of four human genes that form transmembrane proteins [1-3]. When heteroexpressed in HEK293 cells, all four human Bestrophin genes produce novel and unique Cl^- anion currents [4,5]. Mutations in one family member, Bestrophin-1 (*BEST1* or *VMD2*), have been linked to five distinct ocular pathologies in humans: an autosomal dominant form of juvenile blindness known as Best vitelliform macular dystrophy, adult-onset foveomacular vitelliform dystrophy, autosomal dominant vitroretinochoroidopathy, autosomal dominant MRCS (microcornea, rod-cone dystrophy, early-onset cataract, and posterior staphyloma), and autosomal recessive bestrophinopathy (see [1,2,6] and reviews [7-9]). Expression of Best1 is particularly high in the retina and retinal pigment epithelium, consistent with a role in visual system. However, Best1 mRNA expression have also been detected in testes, spinal cord, and the brain [2,3,10]. Emerging studies suggest that in the brain Best1 forms glial Cl^-/anion channel and is responsible for release of neurotransmitters GABA and glutamate from astrocytes [10-13]. Best1-mediated GABA release has been shown to contribute to tonic inhibition of neuronal activity in cerebellum and perhaps other brain regions [11].

Homologous Bestrophins genes have been identified throughout the animal kingdom, including in the model organisms *Drosophila melanogaster* and *Caenorhabditis elegans* [7]. A high degree of conservation is seen in the N-terminal portion of all Bestrophin proteins, particularly in areas composed of hydrophobic amino acids that are hypothesized to encode transmembrane domains [7,14]. GenBank lists two principal human Best1 variants, Best1V1 and Best1V2, whose protein products differ in both the N- and C-termini due to alternative splicing (first reported by Wistow et al. [15]). While the first exon is common to both variants, it does not contain a translational start site. As translation initiates at a start codon in either exon 2 or exon 3, depending on alternative splicing, inclusion of exon 2 in the Best1V1 variant results in a protein with a longer, unique N-terminus. The amino acid sequence encoded by exon 2 is thought to form a transmembrane domain and lack of this fragment in Best1V2 may have important functional consequences [5,16]. Alternative splicing at the C-terminus of Best1V2 replaces the terminal 5 amino acids of Best1V1 with a unique 84-amino acid sequence. The C-terminus of canonical Best1V1 variant, which is predicted to be located in the cytoplasm, has been shown to play numerous roles. It contains a putative calcium-sensing domain, and both truncations or point mutations in this domain can dramatically reduce Ca^{2+} activated Cl^- currents in heteroexpression systems [17,18]. Furthermore, it has been reported that the N- and C-termini of the Best1 protein allow for inter-domain interactions and binding [19]. In the latter study, the authors proposed that Best1 multimerization via the N-C-termini interactions is critical for channel function. The functional effects of alternative splicing of the C-terminus are not known.

In the present study, we cloned several Best1 splice variants from normal and malignant human glial cells. In addition to the previously reported Best1V1 and Best1V2 isoforms, we identified a novel Best1V1 splice variant lacking exon 2 (Best1V1Δex2). This splice variant allowed us to explore the functional significance of the N- and C-terminal portions of the Best1 protein. With this purpose, we heteroexpressed Best1V1, Best1V2, and the novel Best1V1Δex2 in HEK293 cells and compared their ability to form ion channels.

Surprisingly, Best1V1 and Best1V1Δex2, but not Best1V2, generated Ca^{2+}- activated Cl^{-} channels. These results indicate that the exon 2-encoded N-terminus is not essential for formation of functional Ca^{2+}-activated Cl^{-} channel. In contrast, the cytoplasmic C-terminus appears to play a critical role, likely via its impact on protein stability.

Experimental

Cell cultures

HEK293 cells (ATCC, passage unknown), human glioblastoma cells U251-MG (gift of Dr. M.G. Kaplitt, Cornell University, New York, NY; passage unknown), retinal pigment epithelium cell line ARPE-19 (gift of Dr. S. Temple, NY Neural Stem Cell Institute, Rensselaer, NY; passage unknown), and primary human astrocytes (ScienCell Research Laboratories, Carlsbad, CA, passages 2-4), were cultured in DMEM medium supplemented with 10% fetal bovine serum (FBS), 50 U/ml penicillin and 50 μg/ml streptomycin. Cells were grown at 37°C in a humidified atmosphere of 5% CO_2/95% air. Cell culture medium was replaced twice a week, and cells were passaged as necessary using recombinant protease TrypLE Express. All culture reagents were from Life Technologies/Invitrogen (Carlsbad, CA).

Primary glioblastoma cells were prepared from surgical samples of pathologically confirmed glioblastoma multiforme. All relevant procedures have been carried out in adherence to the Declaration of Helsinki of the World Medical Association. Tissue was obtained directly from the surgical suite under a protocol approved by the Albany Medical Center Institutional Review Board and with written patient consent. Tumor tissue (~200-300 mg) was washed twice with ice-cold Ca^{2+}-, Mg^{2+}-free phosphate buffered saline (PBS, pH 7.4), minced to small pieces and treated with a solution of 0.125% Trypsin/0.015% EDTA in PBS containing 250 μg/ml DNAse I. After brief digestion, tissue fragments were triturated using a fire-polished glass Pasteur pipette, and the resulting cell suspension was filtered through a Nylon cell strainer (70 μm, BD Falcon, Bedford, MA, USA). Cells were grown in T75 cell culture flasks in DMEM plus 20% FBS supplemented with 100 U/ml penicillin, and 100 μg/ml streptomycin at 37°C in a humidified atmosphere containing 95% air and 5% CO_2. The astroglial origin and homogeneity of the resulting cultures were previously confirmed by immunocytochemical staining for glial fibrillary acidic protein (anti-GFAP monoclonal antibody, G3893, Sigma-Aldrich, St. Louis, MO) [20].

Cloning of Bestrophin-1

mRNA was isolated from cell cultures using the RNAqueous-4PCR kit (Applied Biosystems/Ambion, Austin, TX) according to the manufacturer's instructions. Concentrations of mRNA were quantified using a NanoDrop 1000 (Thermo Fisher Scientific, Wilmington, DE). mRNA was converted to cDNA using the iScript cDNA Synthesis kit (BioRad Laboratories, Hercules, CA) following the manufacturer's instructions, and using proportion of one μg mRNA per 20 μl reaction mix The primers used for amplification in RT-PCR were purchased from Life Technologies/Invitrogen. The sequence of the upstream primer located in exon 1 was TGTTGACTGCAGCCCGGTATTCAT. This was combined with a downstream primers

specific for either Best1V1 (ACAGCTGTATGGCTGTGACTGGAT) or Best1V2 (TGGTCAGCACAA CCTCATCTTCCT). Amplification was performed using 5 PRIME MasterMix (5 PRIME, Inc., Gaithersburg, MD). The resulting PCR products were separated on an agarose gel and isolated using Gel Extraction Kit from Qiagen-USA (Valencia, CA). Cloning was performed using the TA Cloning Kit (Life Technologies/Invitrogen) per manufacturer's instructions. Unique clones were initially identified by restriction digestion and subsequently commercially sequenced (Genewiz, South Plainfield, NJ).

Transient transfection of Best1-containing vectors

For expression studies, two canonical Best1 clones, Best1V1 (catalogue #SC310244), and Best1V2 (SC325224) were purchased from Origene (Rockville, MD). Additionally, C-terminus myc/DDK tagged versions of both these proteins, Best1-DDK (RC214156) and Best1V2-DDK (RC227442), were also acquired from Origene. The new Best1V1Δex2 splice variant was subcloned into pcDNA3 (Life Technologies/Invitrogen) for expression studies. Best1V1Δex2-DDK was generated by replacing the N-terminus of Best1V1-DDK with the N-terminus of Best1V2-DDK. Proper cloning was confirmed by sequencing.

HEK293 cells were grown to 10% confluence on 12×12 mm glass coverslips for electrophysiological studies, or 50% confluence in 60 mm plastic Petri dishes for Western blotting. Cells were transfected using Lipofectamine 2000 (Life Technologies/Invitrogen) according to the manufacturer's instructions, using Best1 cDNA together with pMAX eGFP expressing plasmid (Lonza, Allendale, NJ). Co-transfection with eGFP was utilized to assess transfection efficacy and select cells for electrophysiological experiments. The transfected cells were additionally grown for 48 hrs at 37°C before used for Western blot analysis or electrophysiological experiments.

Whole cell electrophysiology

Whole-cell recordings from transfected cells were performed at room temperature (20°C). Extracellular and intracellular solutions were formulated to isolate Ca^{2+}-activated Cl^- currents. Bath solution contained (in mM): 140 NaCl, 10 TEA-Cl, 2 $CaCl_2$, 1 $MgCl_2$, 10 Glucose, and 10 Hepes (pH 7.4 adjusted by NaOH). The pipette solution contained (in mM): 90 NMDG, 60 NMDG-Cl, 50 aspartic acid, 3 $MgCl_2$, 3 ATP-Na_2, 5 EGTA-Na_4, 10 Hepes (pH 7.2). Free Ca^{2+} concentration in the pipette solution was kept nominally 0, or adjusted to 1 μM by adding $CaCl_2$. Free Ca^{2+} levels were calculated using CaBuf software (G. Droogmans, KU Leuven, Leuven, Belgium). Patch electrodes were fabricated from borosilicate glass capillaries using a micropipette puller (P-97, Sutter Instruments, Novato, CA), and had a resistance of 2.5-3.5 MΩ when filled with pipette solution. Series resistances were ≤15 MΩ. Currents were recorded with an Axopatch 200B amplifier (Axon Instruments, Foster City, CA). pCLAMP software (version 9.2, Axon Instruments) was used for command pulse control, data acquisition, and analysis. Current signals were filtered at 2 kHz using a four-pole Bessel filter and digitized at 4 kHz. Two electrophysiological protocols were used to record Best1 currents: step pulses from −100 mV to +100 mV in 20 mV increments and voltage ramps from −100 mV to +100 mV. Current densities in all groups of cells were calculated by measuring steady state currents at +100 mV and normalizing them to membrane capacitance of each individual cell. Reversal potentials for currents under all

experimental conditions were determined empirically and compared to Cl^- equilibrium potential. The Cl^- equilibrium potential was calculated using the online tool (http://www.physiologyweb.com/calculators/) based on the Nernst equation and assuming complete exchange of Cl^- between pipette and the cell cytosol.

Western blot analysis

Protein expression was assessed by Western blot analysis using two specific antibodies for Bestrophin-1: mouse monoclonal anti-Best1 (E6-6, Abcam, Cambridge, MA, cat. # ab2182) or mouse polyclonal anti-VMD2/Best1, (Abnova, Taipei, Taiwan, cat. # H00007439-B01). A monoclonal antibody against DDK (Origene) was additionally used to detect the DDK tagged Best1V1, Best1V1Δex2, and Best1V2. HEK293 cells were transfected with various Best1 clones and 48 hours later lysed with 2% SDS plus 8 mM EDTA. The lysates were immediately further diluted with a reducing Laemmli buffer. The total protein content in cell lysates was determined using a colorimetric BCA assay kit (Thermo Fisher Scientific/Pierce, Rockford, IL). Proteins were separated on a 10% polyacrylamide gel (Thermo Fisher Scientific/Pierce) and transferred onto an Immun-Blot PVDF membrane (Bio-Rad). The membranes were blocked with 5% non-fat milk in a Tris-buffered saline solution (TBS) containing 0.1% Tween-20 (TBS-Tween), and incubated overnight with primary antibody (as specified) at 1:1,000 dilution. Membranes were then washed with TBS-Tween to remove unbound antibodies prior to incubation with a horseradish peroxidase (HRP)-conjugated secondary antibodies (1:10,000, GE Healthcare, Piscataway, NJ). Immunoreactive signal was detected using an ECLplus reagent (GE Healthcare) in a luminescent image analyzer LAS-4000 (FujiFilm Medical Systems, Stamford, CT).

Surface Protein Biotinylation

HEK293 cells were grown in T75 flasks and transfected with Best1 isoforms using Lipofectamine 2000 as described above. At 48-60 hrs after transfection, cell surface proteins were labeled using a biotinylation kit (Thermo Fisher Scientific/Pierce) per manufacturer's instructions. Biotinylated proteins were identified by Western blot analysis as described above. As a control, we probed for presence of major cytosolic protein, actin, among purified biotinylated proteins.

Statistical Analyses

All data in this study are presented as mean values ± standard error (SE) with the number of independent experiments or cells included in electrophysiological analyses indicated in figures or figure legends. Statistical difference between experimental groups was determined by one-way ANOVA and post hoc Bonferroni or Tukey test for multiple comparisons unless stated otherwise. p values <0.05 were accepted as statistically significant. Prism 5 (GraphPad Software, San Diego, CA) or Origin 8.1 (Origin Labs, Northampton, MA) were used for statistical analyses.

Results

Cloning of Best1 splices variants from human primary astrocytes, primary glioblastoma cells and retinal pigment epithelium cells

To identify splice variants of Best1 expressed by glial cells, RT-PCR was performed using cDNA from normal human primary astrocytes, two primary human cultures derived from surgical glioblastoma specimens, and the glioma derived cell line U251-MG. Amplification was performed using a primer in exon 1 upstream to the translational start sites paired with downstream primers specific for either the Best1V1 or Best1V2 C-terminus. The previously reported isoforms, Best1V1 (GenBank NM_004183) and Best1V2 (NM_001139443) were both identified (Fig. 1A). However, we also isolated a novel Best1V1 isoform lacking exon 2 (Best1V1Δex2, GenBank JQ954696) from U251-MG cells, human primary astrocytes, and one of the primary glioblastoma cultures (Fig. 1A). The isolation of this splice variant from multiple cell lines suggests that alternative splicing of exon 2 in Best1V1 is a naturally occurring phenomenon in both normal and malignant glial cells. The predicted protein structures for three alternatively spiced variants are presented in Fig. 1B, that was prepared based on the protein model proposed by Milenkovic et al. [16].

To determine if the Best1V1Δex2 isoform is unique to glial cells, we cloned isoforms of Best1 expressed in the cell line ARPE-19, a retinal pigment epithelium (RPE) derived cell line that maintains many properties of differentiated RPE cells [21]. Using the primers described above, we were able to isolate the canonical isoforms, Best1V1 and Best1V2, as well as Best1V1Δex2. These findings demonstrate that the novel splice variant is not unique to cells of the glial lineage.

Heteroexpression and characterization of two canonical Best1 variants

Although several different splice variants of Best1 have been deposited in GenBank, expression and functional studies have been restricted to the Best1V1 isoform and its naturally occurring mutants (reviewed in [7]). We, therefore, heteroexpressed both Best1V1 and Best1V2 in HEK293 cells to compare the ability of the two canonical splice variants to produce functional protein. Heteroexpression of Best1V1 resulted in the appearance of an immunoreactive band that was close to the predicted molecular weight of 68 kD for the Best1V1 protein (Fig. 2A). When Best1V2 was heteroexpressed under identical conditions, we were unable to detect a signal on Western blot using the same monoclonal antibody (Fig. 2A).

As Best1V2 protein expression has not been reported in the literature, we performed Western Blot analysis using two additional detection reagents. We first utilized a commercially available polyclonal antibody raised against the full length Best1V2 (Abnova). This antibody detected an immunopositive band for Best1V1, and two weaker bands for Best1V2. The upper Best1V2 band was of similar molecular weight to Best1V1. The lower Best1V2 band was ∼9-10 kD lighter (Fig. 2B). To further confirm that both bands are the products of the Best1V2 gene, we heteroexpressed commercially available Best1V2 fusion protein (Origene) containing the DDK and myc epitopes at the C-terminus. When probed with the polyclonal antibody raised against Best1V2, we again detected two

bands (Fig. 2B). The molecular weights of these bands were higher than the corresponding bands seen for Best1V2, consistent with the presence of the fusion epitopes. When probed with an anti-DDK antibody, the same two immunoreactive bands were found as with the Best1 polyclonal antibody (Fig. 2C). Altogether, these results unequivocally show that Best1V2 protein can be heteroexpressed in mammalian cells. The currently available antibodies do not permit for determination of the relative abundance or stability of Best1V2 protein as compared to Best1V1.

Channel formation by two known Best1 splice variants in HEK293 cells

To our best knowledge, all prior studies demonstrating that Best1 encodes a Ca^{2+}-activated Cl^- channel have been performed using wild type Best1V1 or its mutant forms (reviewed in [7], see also [19]). As similar studies have not been done with Best1V2, we expressed Best1V1 and Best1V2 in HEK293 cells to determine if both isoforms were capable of forming functional channels. These experiments were performed under conditions allowing for isolation of Cl^- currents, with the Cl^- equilibrium potential set at ~ -21 mV (see Methods).

Under Ca^{2+}-free conditions, wild type HEK293 cells showed very low current densities, $\sim$10 pA/pF, and a current reversal potential that was $\sim$10 mV more positive than the Nernst potential for Cl^- (Fig. 3G, Supplemental table 1). Thus, as expected, basal Cl^- conductance (I_{Cl}) in HEK cells was very low and, as a result, partially obscured by non-selective cation and/or leak currents. Addition of Ca^{2+} into pipette solution produced no significant changes in the amplitude of the wild type currents, but moved the reversal potential somewhat closer to that of Cl^- (Fig. 3G, Supplemental Fig. 1, and Supplemental table 1). When the inhibitor of Ca^{2+}-activated Cl^- channels niflumic acid was added to the bath solution, it produced a very small but statistically significant reduction in I_{Cl} (Fig. 3G, Supplemental table 1). However, the effect of niflumic acid was independent of $[Ca^{2+}]_{pipette}$, and thus unlikely to be mediated by Ca^{2+}-activated Cl^- channels (see Discussion for additional details).

Overexpression of Best1V1 produced strong augmentation in the transmembrane currents under Ca^{2+}-free conditions, with further significant increases seen upon inclusion of 1 μM free Ca^{2+} into the pipette solution (24.4±6.1 pA/pF, p=0.044 and 75.0±11.1 pA/pF, p<0.001, for Ca^{2+}-free and Ca^{2+}-containing conditions, respectively, as compared to 12.2±2.2 pA/pF current densities registered in the wild type cells, Fig. 3B, D-F, H, see Supplemental Table 1 and Supplemental Fig. 1 for extended analysis and representative traces). The Ca^{2+}-dependent current component in the Best1V1-expressing cells were completely suppressed by addition of 200 μM niflumic acid into bath solution (75.0±11.1 pA/pF vs. 26.0±11.3 pA/pF, p=0.036, Fig. 3H; see also Supplemental table 1 and Supplemental Fig. 2 for extended analysis and representative traces), and this effect was accompanied by positive shift in the current reversal potential, strongly supporting involvement of Ca^{2+}-activated Cl^- channels. Altogether, these data suggest that overexpression of Best1V1 gives a rise to Ca^{2+}-dependent Cl^- conductance, but may also increase nonselective plasmalemmal conductance (see Discussion for additional details).

In striking contrast to Best1V1, transfection of HEK293 cells with Best1V2 did not produce a statistically significant increase in transmembrane currents, nor did it lead to the

appearance of a Ca^{2+}- and niflumic acid-sensitive Cl^- current component (Fig 3C, I, Supplemental table 1). Furthermore, the I_{Cl} in the Best1V2 heteroexpressing cells was not statistically different from the wild type controls

Functional characterization of the novel Best1 splice variant, Best1V1Δex2

Best1V1 and Best1V2 differ at both the N- and C-termini due to alternative splicing (see Fig. 1B for reference). Comparison of the Best1V1Δex2 isoform to Best1V1 allows for direct assessment of the contribution of the exon 2 encoded N-terminus to Best1 function. When Best1V1Δex2 was heteroexpressed in HEK293 cells, Western blotting using the monoclonal anti-Best1 antibody detected a signal close to the predicted molecular weight of 61 kD (Fig. 4A). Curiously, we also observed a lower molecular weight signal (~9-10 kD). The appearance of an additional band was similar to the results seen upon expression of Best1V2, which also lacks exon 2 (compare to Fig. 2B, C). These findings may suggest that while the exon 2-encoded N-terminus is not critical for protein synthesis, it may play a posttranslational role affecting protein stability.

To determine if Best1V1Δex2 can form functional Cl^- channels, we performed whole cell electrophysiological recordings in HEK293 cells transfected with this isoform. In 5 out 12 recorded Best1V1Δex2-expressing cells, we detected outwardly rectifying Ca^{2+}-activated Cl^- currents (Fig. 4B, C, Supplemental Fig. 1). These currents were quite similar to those observed in Best1V1-expressing cells, and were sensitive to addition of 200 μM niflumic acid (Fig. 4C, D, Supplemental Fig. 2). In the cells showing outwardly rectifying, and Ca^{2+}-sensitive Cl^- currents, the average current density was 40.1.5±6.2 pA/pF in the presence of 1 μM free Ca^{2+}. This was significantly higher than the average current density of 4.6±0.8 pA/pF recorded in Best1V1Δex2-transfected cells under Ca^{2+}-free conditions ($p<0.001$, Fig 4D, Supplemental table 1). Overall, these results demonstrate that the Best1V1Δex2 variant, which lacks the N-terminus encoded by exon 2, is capable of forming functional Ca^{2+}-activated Cl^- channels.

Surface expression of Best1 isoforms

The electrophysiological differences seen in cells expressing the three Best1 isoforms may arise from effects on protein trafficking. Because of a lack of antibodies that recognize Best1V2 with high efficacy, we utilized C-terminus DDK-tagged versions of Best1V1, Best1V1Δex2, and Best1V2, which were heteroexpressed in HEK293 cells. The plasmalemmal proteins were identified by surface protein biotinylation. Consistent with the results of electrophysiological assays, we detected surface biotinylation of both Best1V1-DDK and Best1V1Δex2-DDK (Fig. 5A, B). To control for non-specific biotinylation of cytosolic proteins, the biotinylated fraction was probed with an anti-actin antibody which detected no actin signal (Fig. 5B, see also Supplemental Figure 3). While multiple immunoreactive bands were seen in the clarified crude lysates, only one band corresponding to the predicted molecular weights for each of the Best1 splice variants was isolated from biotinylated fraction. Interestingly, we consistently observed much stronger signal for the biotinylated Best1V1 than that for Best1V1Δex2. This may suggest that Best1V1 is more efficiently trafficked to the surface than Best1V1Δex2, again in agreement with the results of electrophysiological studies. A number of low molecular weight bands seen in the crude

lysates of Best1V1- and Best1V1Δex2-expressing cells likely represent protein breakdown products. Similar results were obtained when untagged Best1V1Δex2 was heteroexpressed and detected using the monoclonal anti-Best1 antibody E6-6 (data not shown).

In contrast to Best1V1 splice variants, we found no evidence for surface expression of Best1V2-DDK in the biotinylated fraction (Fig. 5B). In fact, the crude lysates demonstrated two extremely faint signals for a low-molecular weight product of ∼32-35 kD and an additional ∼60-62 kD band that was closer to the predicted molecular weight of for Best1V2 (signal is indicated by asterisks in Fig. 5B because it is too weak to be seen). The extremely low levels of Best1V2-DDK-immunoreactivity in crude lysates were puzzling considering results of preceding experiments (see Fig. 2B and C). The difference in signal intensity was hypothesized to be due to the conditions used for lysis during protein extraction (2% SDS vs. commercial non-ionic detergent-based lysis buffer optimized for the surface biotinylation assay). Therefore, we additionally tested the remnant pellets obtained after clarification of the biotinylated cell lysates. After the SDS solubilization of pellets, we detected several strong DDK-immunoreactive bands representing the Best1V2 signal (see Supplemental Fig. 3B). Overall, these findings suggest that Best1V2 is not trafficked to the plasma membrane and likely forms misfolded protein, which is targeted for degradation.

Discussion

Alternative splicing of the *BEST1* gene results in multiple potential protein products [15]. When expressed in heterologous systems, “canonical” Best1—Best1V1—produces bona fide Ca^{2+}-activated Cl^- channels [4,5]. In addition Best1V1 has also been shown to regulate activity of the L-type of Ca^{2+}channels, and intracellular Ca^{2+} homeostasis [22-26]. All functional studies to-date have tested only wild type Best1V1 or its clinically relevant mutants (reviewed in [7]). Prior to the present work, it was unclear if the other gene products arising from alternative splicing of Best1 could be successfully translated into protein, or if they are functionally relevant. Discovery of the unique Best1V1Δex2 allowed us to analyze the relative impact of the *BEST1* gene product splicing in N- and C-terminal regions on protein translation and function. We found for the first time that the previously reported Best1V2 mRNA can be translated into protein in mammalian cells, but is not delivered to cell surface, and possibly misfolded. Thus, Best1V2 cannot form functional plasmalemmal Cl^- channel. Very unexpectedly, we discovered that a naturally occurring isoform missing the N-terminal part of the protein, which is predicted to include the first transmembrane domain, is capable of forming functional Cl^- channel. These results are likely to stimulate further work exploring and modeling the protein structure of not only the clinically relevant hBest1 but also other members of the Best family.

The paradoxical nature of the observation of preserved Cl^- channel function in Best1V1Δex2 calls for thorough verification. To recapitulate, we have three independent lines of evidence corroborating our conclusions. (1) Western blot analysis of Best1V1Δex2-transfected cells clearly showed expression of the Best1 protein band with reduced molecular weight as compared to the canonical Best1V1 (Fig. 4A). The specificity of the immunoreactivity signal was independently confirmed using a DDK-tagged Best1V1Δex2 construct probed with an anti-DDK antibody (Fig. 5B). (2) Delivery of the DDK-tagged

Best1V1Δex2 protein to the plasma membrane was reliably detected using a surface biotinylation assay and a highly specific anti-DDK antibody (Fig. 5B). In controls, there was no indication for non-specific biotinylation of cytosolic proteins as demonstrated by probing purified biotinylated material with an anti-actin antibody (Fig. 5B, Supplemental Fig. 3A). (3) Cells transfected with Best1V1Δex2 showed an outwardly rectifying Cl^- current that appeared to be biophysically distinct from the current produced by heteroexpression of canonical Best1V1 (compare Fig. 3B to Fig. 4B, and also see Supplemental Figs. 1 & 2). This latter current was seen only with Ca^{2+} present in the pipette solution, but not under Ca^{2+}-free conditions, consistent with the idea of heteroexpression of Ca^{2+}-activated Cl^- channel. Importantly, no current similar to Best1V1Δex2 was recorded in >40 wild type cells, mock- and GFP-transfected cells, or cells heteroexpressing Best1V2. Altogether, our electrophysiological experiments make a very strong case for existence of Best1V1Δex2-encoded Cl^- channels, and make it unlikely that the ion currents detected by us either represent a recording artifact or upregulation of the endogenous ion conductance.

Previous studies suggest that there is a high degree of homology in the N-terminal portion of Best1 between species, as well as between the four human Bestrophin family members (Best1-4) [7,14]. Although, the two presently existing topologic models differ on position and orientation of Best1 transmembrane domains, both agree on a cytoplasmic location for the N-terminus with exon 2 encoding the first transmembrane domain [5,16]. The functional significance of the N-terminal domain in Best1 is implied by the fact that a number of known human mutations in the cytosolic N-terminus (e.g., T6P, L21V, W24C, R25Q or R25W), and in the first predicted transmembrane domain (S27R, K30R Y29H, L41P), have been linked to diseases of visual system (University of Regensburg *VMD2* database, reviewed in [7]). Some (but not all) of these mutations dramatically reduce the whole-cell Best1 currents in heteroexpression systems, and/or disrupt N-C terminus interactions [19,27]. The Best1V1Δex2 splice variant is missing the translational start side encoded in exon 2, and consequently lacking the cytosolic N-terminus and the predicted first transmembrane domain. Such a deletion would be expected to strongly influence or completely disrupt Best1 processing, trafficking, and/or function. Our present demonstration that this naturally occurring Best1V1Δex2 truncation forms functional Cl^- channel needs to be further reconciled with the current structural models (see Fig 1B). Since we found that BestV1Δex2 is (i) translated into a stable protein product, (ii) trafficked to the surface, and (iii) forms a functional Cl^- channel, the N-terminal 60 amino acids appear to not be essential for these functions. Furthermore, our findings conflict with the idea that interaction between the cytosolic N- and C-termini is obligatory for the formation of Ca^{2+}-activated Cl^- channels [19].

The trafficking of truncated Best1V1Δex2 protein to cell surface is not unprecedented. Similar phenomenon was reported for an alternatively spliced Best3 protein lacking the N-terminal exons 2, 3 and 6 [28]. One major difference though is that despite being trafficked to the cell surface the truncated Best3 failed to form Cl^- channels or modulate activity of co-expressed wild type Best3 channels [28]. In our assays, we found lower protein expression and apparent reduction in surface delivery of Best1V1Δex2 as compared to the full length Best1V1. Monoclonal anti-Best1 and anti-DDK tag antibodies consistently detected multiple

bands below the predicted molecular weight for Best1V1Δex2. Thus, it is plausible that N-terminus determines or regulates Best1 protein stability and turnover. This idea is indirectly supported by the fact that Best1V2 splice variant, which also lacks exon 2, showed a similar pattern of multiple immunoreactive bands pointing to proteolytic degradation.

The reduced protein stability and surface expression of Best1V1Δex2 can explain why relevant currents were registered only in five out of 12 tested cells. This was in contrast to cells heteroexpressing Best1V1, where more than 80% of the cells showed very large Ca^{2+}-activated Cl^- conductance. Despite the fact that Ca^{2+}-activated Cl^- current was seen only in a subpopulation of Best1V1Δex2-transfected cells, it was very distinct due to its strong outward rectification. On the surface, these findings may suggests that the first predicted transmembrane domain, although not critical for formation of ion channel pore, plays an important role in regulating the biophysical properties of Best1. However, closer inspection of the electrophysiological data indicates that the differences between Best1V1 and Best1V1Δex2 currents may be smaller than they seem. The apparent Best1V1 rectification was reduced by development of additional niflumic acid-insensitive currents, which were essentially linear. The niflumic acid-insensitive current component was preserved under Ca^{2+}-free conditions and in majority of cells had the reversal potential more positive that the Nernst potential for Cl^- (see Supplemental Table 1). Therefore, we speculate that high expression levels of Best1V1 cause “protein overload” and increase non-selective cation or leak currents. In several recordings, the outward rectification of Best1V1 currents was substantially closer to that seen for Best1V1Δex2 (see several examples in Supplemental Fig. 1). Besides rectification, rather similar current amplitudes and kinetics for Best1V1 and Best1V1Δex2 observed in many cells may suggest that truncation of the N-terminus does not cause substantial changes in channel opening probability, activation, or inactivation.

Best1V1Δex2 similarly provided us with a unique opportunity to investigate the functional impact of alterative splicing in the C-terminus. The only difference between Best1V1Δex2 and Best1V2 is in the alternatively spliced exon 11 (see Introduction and Fig. 1B for reference). In the resulting protein product, the terminal five amino acids present in Best1V1 and Best1V1Δex2 are replaced with a unique 84 amino acid sequence. Our finding that Best1V1Δex2 can form a Ca^{2+}-activated Cl^- channel, but that Best1V2 does not, identifies splicing of the C-terminal domain as a critical determinant of Best1 protein function. According to both existing topological models, the C-terminus forms a large cytoplasmic domain [5,16]. This domain has been shown to include sequences that contain putative Ca^{2+} interaction motifs [17]; it has also been proposed to be involved in interdomain interactions and formation of multimeric Best1 channels [19]. Recent publications implicated the C-terminus in functional interaction between Best1 protein and voltage gated Ca^{2+} channels [29], and found that Ca^{2+}/calmodulin-dependent phosphorylation of Drosophila dBest1 and human hBest1 at several putative sites on C-terminus potently regulate Cl^- channel activity [30]. All of the above mentioned amino acid sequences in Best1V1 are preserved in Best1V2. Therefore, it was somewhat surprising to find that Best1V2, unlike Best1V1Δex2, is incapable of forming detectable Ca^{2+}-activated Cl^- channels. We additionally co-expressed Best1V1 and Best1V2 to see if the presence of the latter can modify Cl^- channel function via hypothetical heteromerization, but found no differences in resulting Cl^- current densities or biophysical properties (see Supplemental Table 1). Our surface biotinylation

experiments provided a plausible explanation for these findings: Best1V2 likely forms a misfolded product and cannot be trafficked to the cell surface. Using biotinylation, not only were we unable to detect Best1V2 on cell surface, but the protein was conspicuously absent in the clarified protein lysates and eventually found in the mild detergent-insoluble pellets. Keeping these findings in mind, there is distinct possibility that that human Best1V2 splice variant represents an error of mRNA splicing. We were unable to find reports of alternative splicing of the C-terminus in non-human Best1 homologues, supporting the view that Best1V2 may represent an aberrant gene product.

Understanding of the structure-function relationship in Best1 has been stimulated by clinical findings. As already mentioned, mutations in *BEST1* gene cause multiple forms of macular degeneration, pointing to significance of Best1 in the visual system. The majority (∼90%) of the disease-related Best1 mutations are missense mutations causing loss of endogenous protein or Cl^- channel function when tested in the heteroexpression systems. A number of other clinically relevant mutations result in protein with partially reduced Cl^- channel function, and/or affect protein trafficking to the plasma membrane [27,31]. Yet, there is continued debate as to the role of Best1 as a plasmalemmal Ca^{2+}-sensitive Cl^- channel responsible for the visual system defects and global electrophysiological changes seen in the bestrophinopathies (reviewed in [8,9]). A number of experimental observations contradict the latter idea. Most importantly, deletion of *BEST1* does not dramatically impact the visual system in mice [9]. However, this “silent” Best1 phenotype may be a species-specific phenomenon. A stop codon mutation in the canine Best1 homologue results in canine multifocal retinopathy that recapitulates many aspects of human disease [32]. In this overall context, it is difficult to reconcile our findings of preserved Cl^- channel function in Best1V1Δex2 with previous reports that single amino acid mutations in exon 2-encoded N-terminal region cause partial or complete loss of ion channel function. We expect that the novel knowledge and new molecular tools produced in the present work will stimulate further structural modeling of human Best1 and other members of Bestrophin family. Since Best1V1Δex2 was initially cloned from primary human astrocytes and primary glioblastoma cells, it will be also interesting to explore the levels of its endogenous expression and its potential relevance for glial cell physiology

In summary, our results define the impact of alternative splicing on Best1 protein function. The N-terminal part of the protein was previously thought to be critical for formation of fully active Cl^- channels, possibly via the inter-domain interactions between the N- and C-termini. Our discovery that Best1V1Δex2 forms Ca^{2+}-activated Cl^- channels call this into question. Instead, the N-terminus appears to play a role in regulating protein stability and/or trafficking. We also found that alternative splicing of the C-terminus in Best1V2 prevents this protein from trafficking to the plasma membrane and formation of Ca^{2+}-activated Cl^- channel, likely due to misfolding and degradation.

Supplementary Material

Refer to Web version on PubMed Central for supplementary material.

Acknowledgments

We are grateful to Dr. Michael G. Kaplitt of the Weill Cornell Medical College, Cornell University, New York, NY and Dr. Sally Temple of the New York Neural Stem Cell Institute, Rensselaer, NY for gift of U251-MG and ARPE-19 cell lines, respectively.

Funding: This study was supported in part by Albany Medical College [translational grant numbers 206-465247, 205-465270 (to Y.-H.K. and A.A.M.), 201-311079 (to Y.-H.K.)] and by the National Institutes of Health [grant R01 NS061953 (to A.A.M.)].

References

1. Marquardt A, Stohr H, Passmore LA, Kramer F, Rivera A, Weber BH. Mutations in a novel gene, VMD2, encoding a protein of unknown properties cause juvenile-onset vitelliform macular dystrophy (Best's disease). Hum Mol Genet. 1998; 7:1517–1525. [PubMed: 9700209]
2. Petrukhin K, Koisti MJ, Bakall B, Li W, Xie G, Marknell T, Sandgren O, Forsman K, Holmgren G, Andreasson S, Vujic M, Bergen AA, Garty-Dugan V, Figueroa D, Austin CP, Metzker ML, Caskey CT, Wadelius C. Identification of the gene responsible for Best macular dystrophy. Nat Genet. 1998; 19:241–247. [PubMed: 9662395]
3. Stohr H, Marquardt A, Nanda I, Schmid M, Weber BH. Three novel human VMD2-like genes are members of the evolutionary highly conserved RFP-TM family. Eur J Hum Genet. 2002; 10:281–284. [PubMed: 12032738]
4. Sun H, Tsunenari T, Yau KW, Nathans J. The vitelliform macular dystrophy protein defines a new family of chloride channels. Proc Natl Acad Sci U S A. 2002; 99:4008–4013. [PubMed: 11904445]
5. Tsunenari T, Sun H, Williams J, Cahill H, Smallwood P, Yau KW, Nathans J. Structure-function analysis of the bestrophin family of anion channels. J Biol Chem. 2003; 278:41114–41125. [PubMed: 12907679]
6. Davidson AE, Sergouniotis PI, Burgess-Mullan R, Hart-Holden N, Low S, Foster PJ, Manson FD, Black GC, Webster AR. A synonymous codon variant in two patients with autosomal recessive bestrophinopathy alters in vitro splicing of BEST1. Mol Vis. 2010; 16:2916–2922. [PubMed: 21203346]
7. Hartzell HC, Qu Z, Yu K, Xiao Q, Chien LT. Molecular physiology of bestrophins: multifunctional membrane proteins linked to best disease and other retinopathies. Physiol Rev. 2008; 88:639–672. [PubMed: 18391176]
8. Boon CJ, Klevering BJ, Leroy BP, Hoyng CB, Keunen JE, den Hollander AI. The spectrum of ocular phenotypes caused by mutations in the BEST1 gene. Prog Retin Eye Res. 2009; 28:187–205. [PubMed: 19375515]
9. Marmorstein AD, Cross HE, Peachey NS. Functional roles of bestrophins in ocular epithelia. Prog Retin Eye Res. 2009; 28:206–226. [PubMed: 19398034]
10. Park H, Oh SJ, Han KS, Woo DH, Park H, Mannaioni G, Traynelis SF, Lee CJ. Bestrophin-1 encodes for the Ca^{2+}-activated anion channel in hippocampal astrocytes. J Neurosci. 2009; 29:13063–13073. [PubMed: 19828819]
11. Lee S, Yoon BE, Berglund K, Oh SJ, Park H, Shin HS, Augustine GJ, Lee CJ. Channel-mediated tonic GABA release from glia. Science. 2010; 330:790–796. [PubMed: 20929730]
12. Oh SJ, Han KS, Park H, Woo DH, Kim HY, Traynelis SF, Lee CJ. Protease activated receptor 1-induced glutamate release in cultured astrocytes is mediated by Bestrophin-1 channel but not by vesicular exocytosis. Mol Brain. 2012; 5:38. [PubMed: 23062602]
13. Woo DH, Han KS, Shim JW, Yoon BE, Kim E, Bae JY, Oh SJ, Hwang EM, Marmorstein AD, Bae YC, Park JY, Lee CJ. TREK-1 and Best1 channels mediate fast and slow glutamate release in astrocytes upon GPCR activation. Cell. 2012; 151:25–40. [PubMed: 23021213]
14. Milenkovic VM, Langmann T, Schreiber R, Kunzelmann K, Weber BH. Molecular evolution and functional divergence of the bestrophin protein family. BMC Evol Biol. 2008; 8:72. [PubMed: 18307799]
15. Wistow G, Bernstein SL, Wyatt MK, Fariss RN, Behal A, Touchman JW, Bouffard G, Smith D, Peterson K. Expressed sequence tag analysis of human RPE/choroid for the NEIBank Project: over

6000 non-redundant transcripts, novel genes and splice variants. Mol Vis. 2002; 8:205–220. [PubMed: 12107410]

16. Milenkovic VM, Rivera A, Horling F, Weber BH. Insertion and topology of normal and mutant bestrophin-1 in the endoplasmic reticulum membrane. J Biol Chem. 2007; 282:1313–1321. [PubMed: 17110374]
17. Xiao Q, Prussia A, Yu K, Cui YY, Hartzell HC. Regulation of bestrophin Cl channels by calcium: role of the C terminus. J Gen Physiol. 2008; 132:681–692. [PubMed: 19029375]
18. Kranjc A, Grillo FW, Rievaj J, Boccaccio A, Pietrucci F, Menini A, Carloni P, Anselmi C. Regulation of bestrophins by Ca^{2+}: a theoretical and experimental study. PLoS ONE. 2009; 4:e4672. [PubMed: 19262692]
19. Qu Z, Cheng W, Cui Y, Cui Y, Zheng J. Human disease-causing mutations disrupt an N-C-terminal interaction and channel function of bestrophin 1. J Biol Chem. 2009; 284:16473–16481. [PubMed: 19372599]
20. Motiani RK, Hyzinski-Garcia MC, Zhang X, Henkel MM, Abdullaev IF, Kuo YH, Matrougui K, Mongin AA, Trebak M. STIM1 and Orai1 mediate CRAC channel activity and are essential for human glioblastoma invasion. Pflugers Arch. 2013; 465:1249–1260. [PubMed: 23515871]
21. Dunn KC, otaki-Keen AE, Putkey FR, Hjelmeland LM. ARPE-19, a human retinal pigment epithelial cell line with differentiated properties. Exp Eye Res. 1996; 62:155–169. [PubMed: 8698076]
22. Rosenthal R, Bakall B, Kinnick T, Peachey N, Wimmers S, Wadelius C, Marmorstein A, Strauss O. Expression of bestrophin-1, the product of the VMD2 gene, modulates voltage-dependent Ca2+ channels in retinal pigment epithelial cells. FASEB J. 2006; 20:178–180. [PubMed: 16282372]
23. Yu K, Xiao Q, Cui G, Lee A, Hartzell HC. The best disease-linked Cl^- channel hBest1 regulates Ca V 1 (L-type) Ca^{2+} channels via src-homology-binding domains. J Neurosci. 2008; 28:5660–5670. [PubMed: 18509027]
24. Reichhart N, Milenkovic VM, Halsband CA, Cordeiro S, Strauss O. Effect of bestrophin-1 on L-type Ca^{2+} channel activity depends on the Ca^{2+} channel beta-subunit. Exp Eye Res. 2010; 91:630–639. [PubMed: 20696156]
25. Neussert R, Muller C, Milenkovic VM, Strauss O. The presence of bestrophin-1 modulates the Ca^{2+} recruitment from Ca^{2+} stores in the ER. Pflugers Arch. 2010; 460:163–175. [PubMed: 20411394]
26. Gomez NM, Tamm ER, Strauss O. Role of bestrophin-1 in store-operated calcium entry in retinal pigment epithelium. Pflugers Arch. 2013; 465:481–495. [PubMed: 23207577]
27. Milenkovic VM, Rohrl E, Weber BH, Strauss O. Disease-associated missense mutations in bestrophin-1 affect cellular trafficking and anion conductance. J Cell Sci. 2011; 124:2988–2996. [PubMed: 21878505]
28. Srivastava A, Romanenko VG, Gonzalez-Begne M, Catalan MA, Melvin JE. A variant of the Ca^{2+}-activated Cl channel Best3 is expressed in mouse exocrine glands. J Membr Biol. 2008; 222:43–54. [PubMed: 18414923]
29. Milenkovic VM, Krejcova S, Reichhart N, Wagner A, Strauss O. Interaction of bestrophin-1 and Ca^{2+} channel beta-subunits: identification of new binding domains on the bestrophin-1 C-terminus. PLoS ONE. 2011; 6:e19364. [PubMed: 21559412]
30. Duran C, Chien LT, Hartzell HC. *Drosophila* Bestrophin-1 currents are regulated by phosphorylation via a CaMKII dependent mechanism. PLoS ONE. 2013; 8:e58875. [PubMed: 23554946]
31. Davidson AE, Millar ID, Burgess-Mullan R, Maher GJ, Urquhart JE, Brown PD, Black GC, Manson FD. Functional characterization of bestrophin-1 missense mutations associated with autosomal recessive bestrophinopathy. Invest Ophthalmol Vis Sci. 2011; 52:3730–3736. [PubMed: 21330666]
32. Guziewicz KE, Slavik J, Lindauer SJ, Aguirre GD, Zangerl B. Molecular consequences of BEST1 gene mutations in canine multifocal retinopathy predict functional implications for human bestrophinopathies. Invest Ophthalmol Vis Sci. 2011; 52:4497–4505. [PubMed: 21498618]

Abbreviations

Best1	Bestrophin 1
Best1V1/Best1V2	splice variants 1 and 2 of the *BEST1* gene product
Best1V1Δex2	splice variant 1 of Best1 missing exon 2
IR	immunoreactivity
RPE	retinal pigment epithelium
WT	wild type

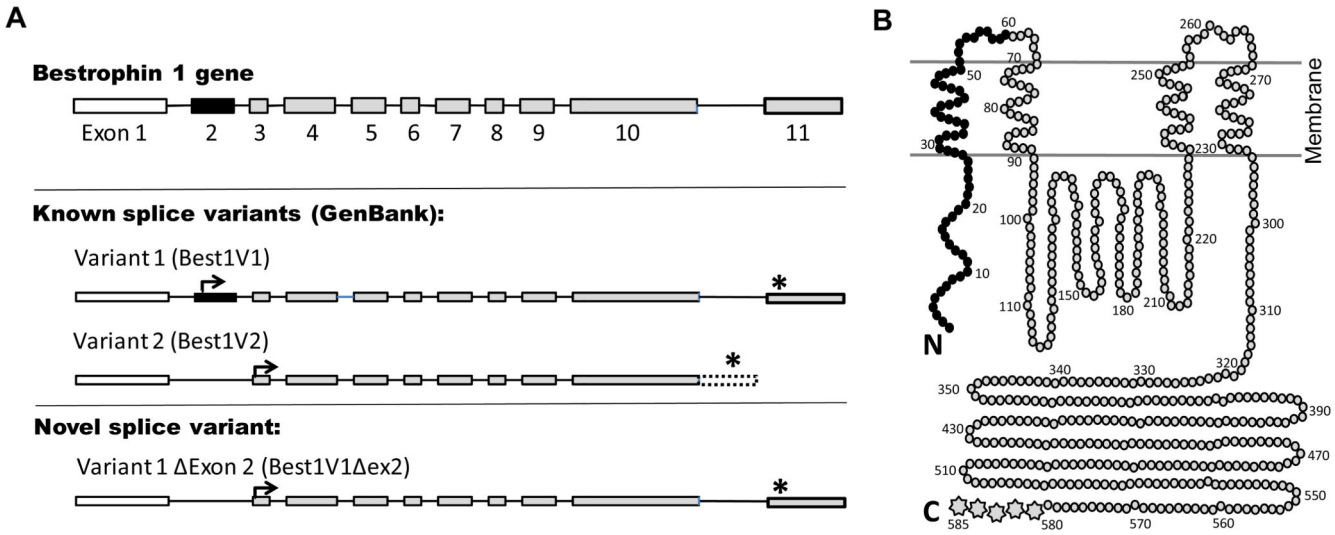

Figure 1. Schematic representation of the Bestrophin-1 gene splice variants (*A*) and their predicted protein products (*B*)

A, The Best1 gene consists of 11 exons. The Best1V1 splice variant (NM_004183) is composed of all 11 exons, with initiation of translation (arrow) in exon 2 and termination of translation (asterisk) in exon 11. In Best1V2 (NM_001139443), exon 2 (solid black) is removed due to alternative splicing, and translation is initiated from a start codon in exon 3. Additionally, Best1V2 does not splice out the intron between exons 10 and 11, and the C-terminus is encoded by translation into the intronic sequence (open box with doted border). The newly cloned Best1V1Δex2 (GenBank accession number JQ954696), is similar to Best1V1 except that it is missing exon 2. ***B***, The Best1 protein model proposed by Milenkovic et al. [16]. This model depicts the predicted membrane topology of canonical Best1V1. In Best1V1Δex2, the first 60 amino N-terminal acids (solid black) are missing. In Best1V2, the first 60 N-terminal amino acids (black) are missing, and the last five amino acids on C-terminus (multipoint stars) are replaced with unique 84 amino-acid sequence.

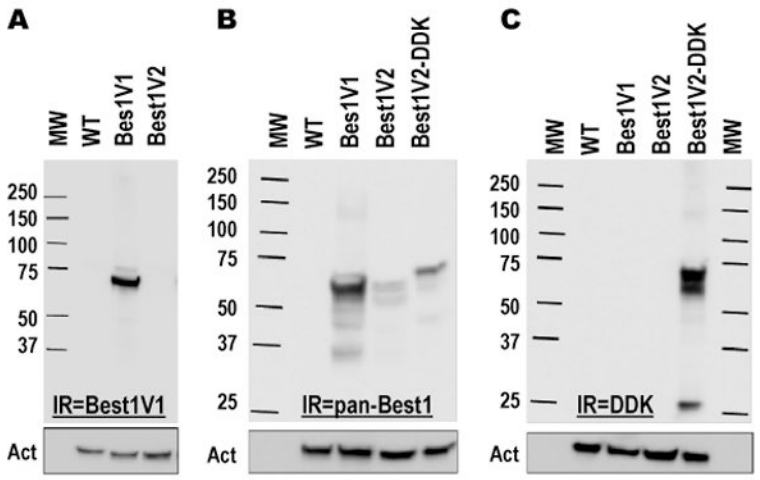

Figure 2. Western blot analysis of previously cloned splice variants of Best1 heteroexpressed in HEK293 cells

A, Best1V1 and Best1V2 were heteroexpressed in HEK293 cells and probed with a monoclonal anti-Best1V1 antibody. ***B***, Best1V1, Best1V2, and Best1V2 with a DDK epitope fused to the C-terminus (Best1V2-DDK) were heteroexpressed in HEK293 and probed with a polyclonal antibody recognizing Best1V1 and Best1V2. ***C***, The same cell lysates as in *B* were probed with an anti-DDK antibody in order to assure specificity of the Best1V2 signal. For all Western blots the membranes were stripped and reprobed with a monoclonal anti-actin antibody to assess equality of loading (shown in boxes below). The figures are representative images of at least three Western blots performed in three independent cell transfections. Abbreviations: MW, molecular weight standards; WT, lysates prepared from mock-transfected (wild type) cells; Act, actin immunoreactivity. IR = immunoreactivity.

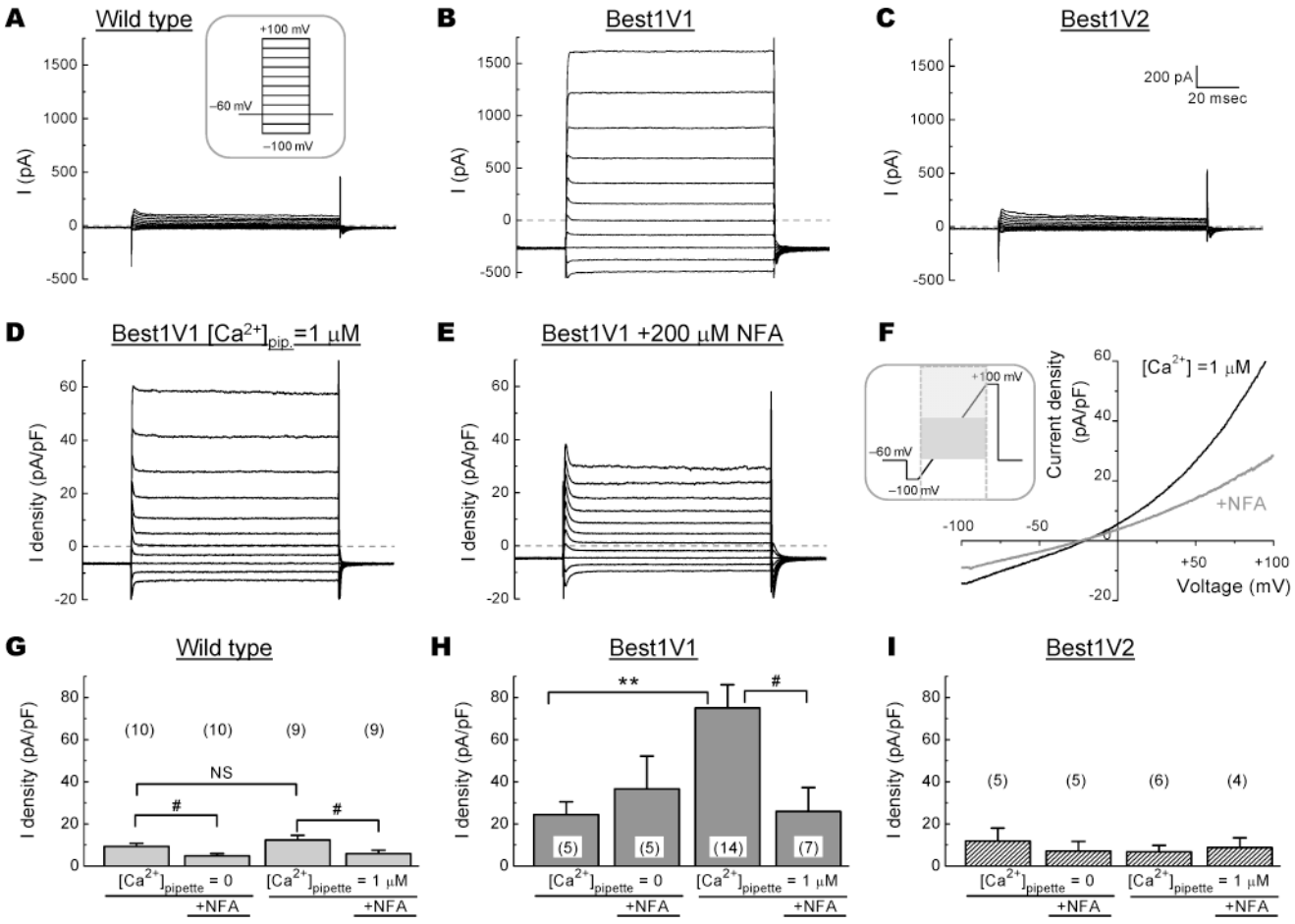

Figure 3. Electrophysiological characterization of canonical splice variants of Best1 heteroexpressed in HEK293 cells

A-C, Representative traces of chloride currents in response to step pulses from -100 mV to +100 mV in 20 mV increments in non-transfected (Wild Type) cells and HEK cells with heterologous expression of Best1V1 or Best1V2. ***D-E***, Representative traces showing the current-voltage relationship of heteroexpressed Best1V1 channels in the absence and presence of 200 μM niflumic acid (NFA). ***F***, The I-V plot demonstrating effect of niflumic acid on Cl^- currents in Best1V1-expressing cells. ***G-I***, Summary of the average Cl^- current densities in non-transfected HEK cells (***G***) and HEK cells heterologously expressing Best1V1 (***H***), or Best1V2 (***I***). Data are the mean values ±SE of average Cl^- current densities recorded from at least two independent cell transfections, with the total number of cells indicated in parentheses. Recordings were performed with $[Ca^{2+}]$ in the pipette solution buffered at 0 or 1 μM, in the presence or absence of 200 μM NFA. **p<0.01, vs. currents recorded at $[Ca^{2+}]_p$=0 μM; #p<0.05 vs. currents recorded in the absence of NFA.

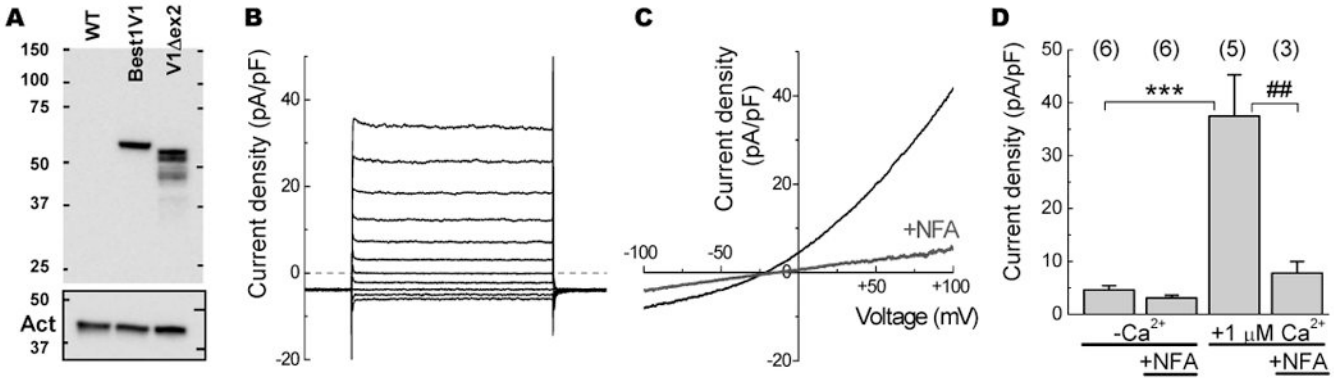

Figure 4. Functional characterization of the novel Best1V1 splice variant missing exon 2 by heterologous expression in HEK293 cells

A, Western blot analysis of Best1V1 and Best1V1Δex2 heteroexpressed in HEK293 and probed with a monoclonal anti-Best1 antibody. Untransfected HEK293 (WT) cell lysates shown as a control for signal specificity. The Western blots membranes were stripped and reprobed with a monoclonal anti-actin antibody to compare protein loading (shown in box below). The figure is a representative image of three Western blots in independent cell transfections. ***B***, Representative traces of Best1V1Δex2-mediated Cl^- currents recorded in response to step pulses from −100 mV to +100 mV in 20 mV increments. ***C***, Representative traces showing the current-voltage relationship of heteroexpressed Best1V1Δex2 channels in the absence and presence of 200 μM niflumic acid (NFA). ***D***, Summary of the electrophysiological recording performed in HEK293 cells expressing Best1V1Δex2. Data are the mean values ±SE of average current densities recorded with $[Ca^{2+}]$ in the pipette solution buffered at 0 or 1 μM, in the presence or absence of 200 μM NFA. The recordings were done in two independent cell transfections, with the number of cells indicated above each bar. Not all Best1V1Δex2-trensfectected cells showed Ca^{2+}-sensitive Cl^- currents (see text for further details). ***$p<0.001$, vs. currents recorded at $[Ca^{2+}]_{pipette}$ = 0 μM; $^{\#\#}p<0.01$ vs. currents recorded in the absence of NFA.

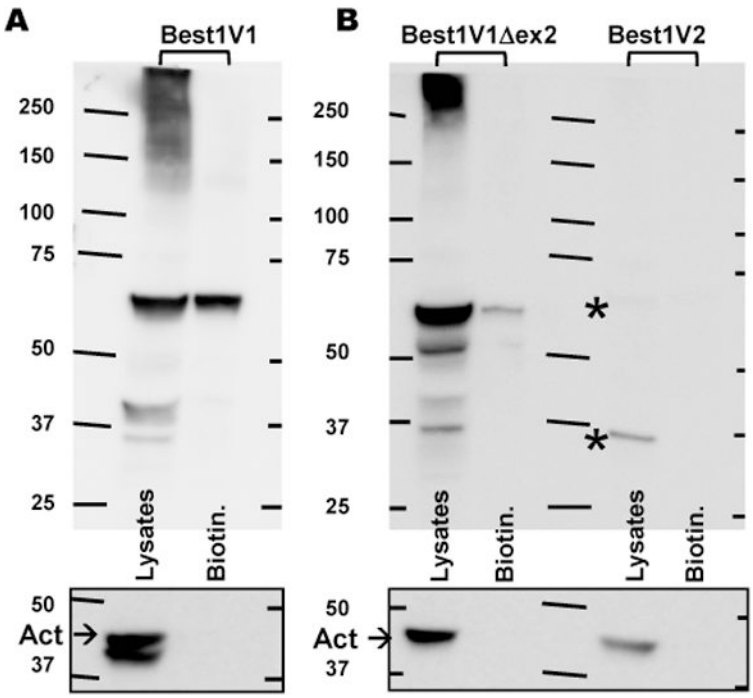

Figure 5. Biotinylation assay of the surface protein expression for three distinct splice variants of Best1 expressed in HEK293 cells

A, Western blot analysis of precipitated biotinylated fraction and the crude cell lysates in HEK293 cells expressing the DDK-tagged Best1V1. Representative of four blots. Because of the difference in the expression levels/intensity of the signal, Best1V1-DDK has been probed separately from Best1V1Δex2-DDK and Best1V2. ***B***, Western blot analysis of biotinylated (surface) material and the crude cell lysates in HEK293 expressing Best1V1Δex2-DDK and Best1V2-DDK. Representative of three blots. Asterisks in (B) indicate two very weak immunoreactive bands in cells expressing Best1V2-DDK. Boxes below each panel show actin immunoreactivity on the same membrane after stripping. These controls show lack of cytosolic proteins in biotinylated fraction.